博士論文

論文題目　Analysis of the turnover mechanism of the proteasome

（プロテアソームのターンオーバー機構の解析）

氏名　　冨田　拓哉

Abstract

The proteasome is proteolytic machinery at the center of regulated protein degradation, which participates in various cellular processes. Besides, human diseases such as autoinflammation and neurodegeration are associated with impaired proteasome activities, emphasizing the importance of research on the regulation of the proteasome activity. However, the turnover mechanism of the proteasome itself has not been explored yet. Here, I show that the proteasome undergoes some specific biochemical alterations long after its biogenesis, which is regulated by particular genes. I established a method for purification of old proteasomes and found that the interactions of Txnl1, Usp14, and actin with the proteasome were enhanced and that Rpn3 was specifically phosphorylated when the proteasome got old. In addition, a human whole-genome siRNA screen determined 10 possible genes that were engaged in the turnover of the proteasome. This screen identified responsible genes that regulate the phosphorylation of the old proteasome. These findings will provide a new direction of researches on the proteasome.

Index

Introduction

The 26S proteasome is an enzymatic complex that mainly degrades ubiquitinated proteins[1]. This large protein complex is composed of a central 20S core particle (CP) capped at either one or both ends by 19S regulatory particles (RP)[2]. The 20S CP is responsible for its proteolytic activity and is made up of seven structurally similar α and β subunits (α1–7 and β1–7). The 19S RP plays an important role in the capture of ubiquitinated proteins and consists of six ATPases (Rpt1–6) and multiple non-ATPase subunits (Rpn1–Rpn3, Rpn5–13, and Rpn15). In addition to the constitutive proteasome subunits, proteasome interacting proteins (PIPs) that transiently associate with the proteasome and play auxiliary roles have been identified. For example, the proteasome assembly chaperones PAC1–4, the deubiquitinating enzymes Usp14 and Uch37, and ubiquitin receptors HHR23b and ubiquilins are well-characterized[3–8]. On the other hand, there still remain many PIPs whose functions are unknown, including the thioredoxin-like protein Txnl1[9,10]. Thus, the proteasome activity is regulated by numerous proteins, but there is still room for further investigation.

It is known that the proteasome plays pivotal roles in various cellular events such as cell cycle, transcription, and immune response[11,12]. In addition, it has been reported that a couple of diseases such as cancer and neurodegenerative diseases are associated with aberrant proteasome activity. In multiple myeloma, the expression and the activity of the proteasome are upregulated[13]. Many of neurodegenerative diseases are caused by accumulations of ubiquitinated misfolded proteins[14]. Downregulation of the proteasome activity triggers autoinflammatory disorder[15]. The activity of the proteasome decreases with aging, whereas increased proteasome activity leads to extension of life span and concomitantly prevents from neurodegeneration[16–18]. Therefore, regulation of proteasome activity is important for understanding pathogenesis of human diseases.

Indeed, numerous researches on the regulation of the proteasome have been conducted. For instance, identification of proteasome-interacting proteins, assembly mechanisms of the proteasome complex, and development of proteasome activators and inhibitors have been studied[19,20].

Here, I propose that the turnover of the proteasome itself be engaged in the regulation of proteasome activities. The proteasome is known to be modulated by a number of post-translational modifications, and previous reports suggest that some of those modifications decreased enzymatic activities of the proteasome[21,22]. In addition, the proteasome contains three catalytically active subunits, β1, β2, and β5, but these are replaced

by immunoproteasome subunits β1i, β2i, and β5i when cells are exposed to inflammatory stimuli such as γ-type interferon (IFN-γ)[23]. Thus, it is expected that damaged or unnecessary proteasomes have to be removed and that the regulation of the turnover of the proteasome is important for maintaining cellular homeostasis. Indeed, since the proteasome is a protein complex that has a measurable half-life[24], its turnover must be under control. As there are few studies on alterations of the proteasome after its biogenesis, this study is aimed at clarifying the turnover mechanism of the proteasome, especially with regard to characterization of aged proteasomes and degradation of the proteasome.

To address this issue, this study was conducted by two strategies. The first was to characterize the old proteasome by biochemical approaches. Using genetically engineered mice that express a subunit of the proteasome with an exchangeable tag, the old proteasome was selectively purified. This assay revealed changes in protein-protein interactions, post-translational modifications, and localization of the old proteasome. The second strategy was to identify genes that affect the turnover of the proteasome. The turnover rate of the proteasome was measured in a human whole-genome siRNA screen. As a result, 10 genes that greatly delayed the turnover of the old proteasome were determined. Finally, this screening identified responsible genes for the phosphorylation of the old proteasome, which was observed in the first strategy, suggesting that this phosphorylation is involved in the turnover of the aged proteasome.

Results

Establishment of a method for purification of the old proteasome

To purify the old proteasome, I made use of the Rpn11-Flag/EGFP tag-exchangeable knock-in mice (Fig 1A). Rpn11 is one of the subunits of 19S RP. In the knock-in allele, a sequence encoding Flag epitope was fused to the 3' end of the Rpn11 coding sequence in the exon 12. The modified exon 12 was flanked by two loxP sequences. EGFP tag was also incorporated with the exon 12 of Rpn11. Accordingly, the knock-in allele expresses Flag-tagged Rpn11. Once it is subjected to Cre-recombinase, the region between the two loxP sequences is excised, switching to express EGFP-tagged Rpn11 and stopping expression of Rpn11-Flag. Using this tool, we can purify old proteasomes by Flag tag after expression of Cre-recombinase in the knock-in cells (Fig 1B). After a certain period of time from the expression of Cre-recombinase, proteasomes that incorporate Flag-tagged Rpn11 are considered as the old proteasome, while incorporation of EGFP-tagged Rpn11 is a marker of the new proteasome. In this experiment, Cre-recombinase was expressed by virus transmission into mouse embryonic fibroblasts (MEFs) derived from Rpn11-Flag knock-in mice at a high multiplicity of infection, as EGFP fluorescence was observed from almost all the MEFs by the expression of Cre-recombinase (Fig 1C).

Protein-protein interaction of the old proteasome

Accordingly, MEFs from Rpn11-Flag mice were infected with retrovirus encoding EGFP or Cre-recombinase, and the old proteasome was purified using Flag-tag three days after the virus transmission. To eliminate artifacts caused by artificial tags that may influence on protein-protein interaction and structure of the tagged protein, the old proteasome was not compared with the new proteasome which can be purified using EGFP tag, but with the total proteasome purified using Flag tag from Rpn11-Flag MEFs that were not infected with virus expressing Cre-recombinase (Fig 2A). This showed that the old proteasome did not show alterations in the composition of 20S CP and 19S RP, as revealed by immunoblot analysis of the 20S CP subunit β3 and the 19S RP subunits Rpt6 and Rpn8, and the silver staining of the whole purified proteasomes following SDS-PAGE (Fig 2B and 2C). Note that Rpn11-EGFP, which was newly synthesized after the expression of Cre-recombinase, was slightly detected in the old proteasome complex (Fig 2B). This suggests that the interaction between 20S CP and 19S RP is reversible in cells. However, the contamination of Rpn11-EGFP in the proteasome purified with Rpn11-Flag is so small that we can consider that the Rpn11-Flag

purified proteasome represents nearly the aged proteasomes. I also examined the amount of several proteasome-interacting proteins that bound to the old proteasome. While the deubiquitinating enzyme Uch37 as well as the ubiquitin receptor HHR23b was recruited almost equally to the total and the old proteasome, the thioredoxin-like protein Txnl1, the deubiquitinating enzyme Usp14, and the cytoskeletal protein actin showed enhanced interactions to the old proteasome (Fig 2B). In contrast, the association between ubiquitinated proteins and the old proteasome was reduced (Fig 2B). This may be due to the enhanced interaction with Usp14, which deubiquitinated substrates on the old proteasome.

The old proteasome is oxidized

Since previous reports have suggested that several post-translational modifications may influence enzymatic activities of the proteasome[21,22], the old proteasome was further examined whether it underwent some modifications. As the carbonylation, which is mainly caused by oxidative stress, has been used for an indicator for protein damage[25], protein carbonyls of the total and the old proteasome were visualized by OxyBlot (Fig 2D). This revealed that while the signals from carbonylated residues both in the total and the old 20S CP were not detectable, the old 19S RP showed increased level of carbonylation, suggesting that the proteasome is subjected to oxidative stress damage as it gets old.

Rpn3 at Ser 6 is phosphorylated in the old proteasome

I also analyzed the phosphorylation status because it is one of the most influential post-translational modifications that regulate various intracellular signals and because it has been reported that the proteasome is regulated by a combination of its phosphorylation[21,22]. The purified total and old proteasome were examined by SDS-PAGE containing Phos-tag acrylamide, in which phosphorylated proteins are detected with mobility shift[26]. Although most of the old 19S RP subunits did not show any band shifts by Phos-tag acrylamide, it was found that the mobility of Rpn3 in the old proteasome was specifically hindered, indicating that the old Rpn3 was phosphorylated (Fig 3A).

To determine the phosphorylation site, the bands corresponding the total and the old Rpn3 were excised and digested by trypsin, and analyzed by liquid chromatography tandem mass spectrometry (LC-MS/MS). While almost equal amount of unphosphorylated peptide 202–209 (ALDLVAAK) were detected, Rpn3 in the old proteasome abundantly possessed a phosphorylated peptide 1–8 (MKQEGpSAR) compared with that in the total proteasome, suggesting Ser 6 phosphorylation of Rpn3 in the old proteasome (Fig 3B and 3C). N-terminus

of Rpn3 is supposed to be located on the surface of the proteasome complex[27], and Rpn3 at Ser 6 is highly conserved only in mammals (Fig 3D).

For the confirmation and further studies of the phosphorylation site of the old proteasome, antibodies specific for phosphorylated and unphosphorylated forms of Rpn3 at Ser 6 were generated. In the Phos-tag acrylamide assay, phosphorylation-specific antibodies specifically recognized the shifted band, whereas antibodies specific to unphosphorylated Rpn3 at Ser 6 detected only the bands the mobility of which was not affected by Phos-tag acrylamide (Fig 3E). This demonstrated that the old Rpn3 at Ser 6 was certainly phosphorylated.

Enhanced deubiquitinating activity and normal proteolytic activity of the old proteasome

Since the old proteasome showed alterations in protein-protein interactions and also in oxidation and phosphorylation states, I next examined whether these modifications influenced the enzymatic activities of the old proteasome. The enzymatic activities of the proteasome were assessed by *in vitro* experiments using model substrates. Deubiquitinating activity was measured using a model substrate Ub-AMC. The old proteasome exhibited increased deubiquitinating activity, which might be due to the elevated interaction of Usp14 to the old proteasome (Fig 4A, also see Fig 2B).

Protease activity was evaluated by *in vitro* degradation assay against two substrates that were degraded by the proteasome in an ATP-dependent manner. The degradation rates were measured against ornithine decarboxylase (ODC) and ubiquitinated inhibitor of apotosis-1 (Ub-cIAP1), which have been reported to be degraded by the proteasome in a ubiquitin-independent and -dependent manner, respectively[28,29]. However, the old proteasome did not show impaired protease activities against these native proteins (Fig 4B). The 26S proteasome is known to possess chymotrypsin-like, trypsin-like, and caspase-like activities, and these catalytic activities can be measured by model peptides, Suc-LLVY-MCA, Boc-LRR-MCA, and Z-LLE-MCA, respectively[30]. Also, the activity of 20S CP, which is inactivated when it does not interact with 19S RP nor any activators, can be spuriously measured by Suc-LLVY-MCA when sodium dodecyl sulfate (SDS) is added[30]. Here again, peptidase activities of the old proteasome against these substrates were not compromised (Fig 4C). Thus, the catalytic activities of the old proteasome seemed to be normal, at least estimated by *in vitro* experiments against these substrates.

Decreased nuclear localization of the old proteasome

I further examined the localization of the old proteasome because changes in protein-protein interaction and post-translational modification often affect the subcellular localization of the modified proteins. In the microscopy analysis, Rpn11-Flag MEFs infected with adenovirus expressing Cre-recombinase were immunostained with anti-Flag antibody to visualize the old proteasome, and the new proteasome was observed by Rpn11-EGFP fluorescence (Fig 4D). The viral titer used in this immunofluorescence assay was relatively lower than other experiments in order to simultaneously detect the old, new, and total proteasome. The fluorescence of EGFP-tagged Rpn11 was stronger in the nucleus compared with that in the cytosol, whereas the immunostained old proteasome was less abundant in the nucleus than that in the cytosol. The total proteasome, which was indicated by anti-Flag immunofluorescence of the cell that did not express Rpn11-EGFP, showed higher fluorescence intensity in the nucleus than in the cytosol. These observations suggest that the old proteasome is less prone to be localized in the nucleus.

This view was supported by cell fractionation analysis. The degradation of Rpn11-Flag in the cytosol and nucleus was observed three days after Cre-recombinase was expressed in Rpn11-Flag MEFs (Fig 4E). While the protein level of 19S RP subunit Rpt6 was not affected by the presence of Cre-recombinase, the decrease of Flag-tagged Rpn11 was greater in the nucleus than that in the cytosol. Besides, the expression of the new proteasome observed by EGFP-tagged Rpn11 was higher in the nuclear fraction. These data suggest that the localization of the proteasome is dependent of its age.

Preparation of Rpn11-Halo knock-in HeLa cells for the turnover measurement

Although the old proteasome was biochemically characterized, the process of the turnover, especially of its degradation, was not clarified from these results. Hence, a human whole-genome knockdown screen was performed to investigate the turnover mechanism of the proteasome. This experiment was based on HaloTag technology, which is a protein fusion tag that can be labeled with fluorescent chemical ligands after HaloTag is expressed in cells[31]. To monitor the turnover of the proteasome, knock-in HeLa cells in which Rpn11 is tagged with HaloTag (Rpn11-Halo) have been generated by CRISPR/Cas9 system[32]. Similar with the construct of Rpn11-Flag/EGFP tag-exchangeable knock-in mice, HaloTag was incorporated into the 3' end of the last exon of Rpn11 coding sequence (Fig 5A). Two knock-in clones were selected by puromycin treatment. Their lysates were immunoprecipitated with antibodies against the 19S RP subunit Rpt6, and Rpn11-Halo as well as wild-type Rpn11 was

pulled down with Rpt6, indicating that Rpn11-Halo was surely incorporated into the proteasome complex (Fig 5B). To examine whether the activity and the composition of the proteasome in this knock-in cells was not impaired, lysates of wild-type and Rpn11-Halo knock-in HeLa cells were fractionated by glycerol gradient centrifugation, followed by the measurement of the peptidase activity of the proteasome with Suc-LLVY-MCA as a substrate. The peptidase activities of each fraction were almost identical between wild-type and Rpn11-Halo knock-in cells, suggesting that the function of the proteasome in the knock-in clone was normal (Fig 5C).

To judge whether this Rpn11-Halo knock-in HeLa can be used for the large-scale screen that would monitor the turnover of the proteasome, pulse-chase labeling experiment was performed (Fig 5D). Rpn11-Halo knock-in HeLa cells was labeled with Oregon Green, a green ligand, and subsequently subjected to the blocking ligand to mask unreacted Rpn11-Halo. After a set time, the cells were labeled with TMR, a red ligand, just before cell harvest to detect newly synthesized Rpn11-Halo. Accordingly, the fluorescence of Oregon Green is considered as the signal from the old proteasome, while that of TMR indicates the new proteasome. Although the amount of Rpn11-Halo protein was stable during this pulse-chase experiment, the fluorescence intensity of Oregon Green-labeled Rpn11-Halo was decreased along with the time course, whereas that of TMR-labeled Rpn11-Halo was increased (Fig 5E). Thus, a method for labeling the old and the new proteasome with distinct fluorescent ligands was established.

Whole-genome siRNA screen for the identification of genes that affect the turnover of the proteasome

Using the knock-in cells described above, human whole-genome siRNA screen was performed to identify genes that affect the turnover of the proteasome (Fig 6A). Oregon Green-labeled Rpn11-Halo knock-in HeLa cells were subsequently subjected to the blocking ligand, and seeded onto 384-well siRNA library plates. After incubating for 64 hours, the cells were then labeled with TMR, followed by cell fixation and nuclear staining. The number of the cells and the fluorescence intensities of Oregon Green and TMR per cells, which indicated the old and the new Rpn11-Halo, respectively, were quantified by high-throughput image analyzer.

To identify gene knockdown that delay the turnover of the proteasome, this screening was aimed at selecting siRNA targets that led to an increase specifically in the signal from the old proteasome (i.e., the fluorescence of Oregon Green). For instance,

knockdown of thyroid hormone receptor alpha (THRA), a qualifier of the primary screen, showed great increase in Oregon Green signal, while the cell count and the signal of TMR were not so much altered compared with the knockdown control (Fig 6B). These three parameters were statistically analyzed and qualifiers of the primary screen were chosen by referring Z* score, which is a statistic often used in the data processing of high-throughput screens (Fig 6C)[33]. In practice, approximately 18 thousand targets were narrowed down to 836 genes that marked top 5% Z* score of Oregon Green signal (Z* > 2.5). Original pictures of all those candidates were checked to eliminate false-positives caused by the detachment of the cells and also by scratches in the bottom of the assay plates. Then, candidates that showed higher increase in the Z* score of TMR rather than that in Oregon Green were removed because it is presumed that this case represented the upregulation of the proteasome expression, which was not of interest in this study. Additionally, with consideration of cell counts, I eliminated more candidates the turnover of the old proteasome of which might be delayed due to their poor cell growth rates. Through this procedure, 261 genes were chosen for the secondary screen.

The secondary screen was performed in three ways. First, using the same cell line with the primary screen, the old proteasome was labeled with Oregon Green as done in the primary screen to evaluate reproducibility. Second, the old proteasome was labeled with TMR to eliminate artifacts brought by labeling ligand because labeling efficiency and detectability are different between HaloTag ligands. In these two assays, new proteasomes were not labeled with any ligands because the turnover of the old proteasome was intended for analyses. Finally, in order to select genes that specifically worked on the proteasome, the turnover of the old proteasome was compared with that of other fluorescent protein, Venus. For this experiment, HeLa cells stably transfected with Tet-On inducible Venus were generated. This transfected cell was exposed to doxycycline for a certain period of time to activate the expression of Venus, and after washing out of the doxycycline the turnover of Venus protein was measured also by the high-throughput image analyzer (Fig 7A).

Before comparing the turnover rate of the proteasome with that of Venus, first two of the three assays in the secondary screen using Rpn11-Halo knock-in HeLa cells were statistically analyzed preferentially. siRNA targets that marked high score (Z* > 2.5) both in those two experiments were chosen for the further confirmation assay using flow cytometer, which might be more precise in the quantification of fluorescence intensities. In addition, siRNA targets for several kinase-related genes were additively selected even though their score was not quite high because phosphorylation of the old proteasome had been observed

(see Fig 3). In total, 45 siRNA targets were subjected to the flow cytometer assay. In the same way with the primary screen, the old proteasome was labeled with Oregon Green and the new was with TMR, and their fluorescence intensities were measured by flow cytometer. Again, the turnover of the old proteasome was rather focused. For example, knockdown of erythropoietin receptor (EPOR) resulted in a shift of the scatter plot along the Oregon Green axis, but the plot against TMR axis was not so much altered (Fig 7B).

The result of the flow cytometer assay was compared with the turnover of Venus protein in the secondary screen, and eventually 10 siRNA targets that greatly delayed the turnover of the proteasome were selected (Fig 7C). Although knockdown of AKAP8L did not mark high scores in the flow cytometer assay, this gene was planed for further analyses because global analysis of Rpn3 interactome using mass spectrometry revealed the physical interaction between Rpn3 and AKAP8L protein (Fig 8A and 8B)[34]. On the whole, this screening narrowed down to 10 possible genes that might be engaged in the turnover of the proteasome.

Identification of responsible genes for the phosphorylation of Rpn3

Following the result of the screening, further studies on individual genes were conducted. Among the final 10 qualifiers, two kinase-related genes, AKAP8L and CSNK2A2, were preferentially investigated because those genes possibly participate in the phosphorylation of the old Rpn3. AKAP8L protein works as an anchor for protein kinase A. CSNK2A2 encodes α' subunit of casein kinase II. AKAP11 also encodes a scaffold of protein kinase A, but analysis of AKAP8L was preferred because AKAP8L protein had shown the interaction with Rpn3 as mentioned above.

To examine the change of phosphorylation status of the old Rpn3, knockdown of AKAP8L and CSNK2A2 was performed in Rpn11-Flag MEFs expressed with Cre-recombinase (Fig 9A). Consistent with the view of Fig 2B, the old proteasome showed the enhanced interaction with Txnl1 and Usp14. Surprisingly, knockdown of both AKAP8L and CSNK2A2 reduced the phosphorylation level of Rpn3 at Ser 6 in the old proteasome, suggesting that these two genes are involved in the phosphorylation of the old Rpn3. Moreover, since casein kinase II is known as a constitutively active kinase, casein kinase II α' encoded by CSNK2A2 was overexpressed in Rpn11-Flag MEFs to evaluate its effect on the phosphorylation of Rpn3. Although the physical interaction between the overexpressed casein kinase II α' and the proteasome was not detectable, the enhancement in the phosphorylation of Rpn3 was observed (Fig 9B). This data again suggests the involvement of CSNK2A2 in

the phosphorylation status of Rpn3. Taken together, the whole-genome siRNA screen finally identified genes that delayed the turnover of the proteasome and affected the phosphorylation status of Rpn3, which was altered in the old proteasome.

Discussion

In this study, the methods for turnover measurement and also for purification of the old proteasome were established. The results from this experimental system introduced a novel concept that the proteasome gets old; after the biogenesis of the proteasome complex, its protein-protein interaction, post-translational modifications, and localization change over time. In addition, the high-throughput screen narrowed the list of genes that might be involved in the turnover mechanism of the proteasome. Some of the identified genes were found to be involved in the phosphorylation of Rpn3 in the old proteasome. Nevertheless, there are a lot of issues yet to be solved.

While AKAP8L and CSNK2A2 were found to affect the phosphorylation status of Rpn3, the mechanism was not understood at this point. More specifically, it is unclear whether protein kinase A or casein kinase II directly phosphorylates Rpn3. More detailed analyses such as *in vitro* kinase assay are necessary.

The old proteasome showed enhanced interactions with Txnl1, Usp14, and actin, and Rpn3 at Ser 6 in the old proteasome was phosphorylated. However, the order of these modifications in the process of aging of the proteasome is not clarified. In the siRNA screen, knockdown of TXNL1 and USP14 had little effect on the turnover of the proteasome (data not shown), suggesting that interactions between these molecules and the proteasome did not trigger the turnover process, but were observed as a result of the aging of the proteasome. Although the role of phosphorylated Rpn3 is also unknown, this modification may regulate the turnover of the proteasome because this phosphorylation was affected by AKAP8L and CSNK2A2, which were identified as genes involved in the turnover of the proteasome. The relationship between actin and the proteasome is poorly understood. Although their genetic interaction was reported[35], the physical interaction has not been established. If the old proteasome binds not only to actin but also to cytoskeleton organization, the old proteasome might possibly be transported and sequestrated to a particular subcellular compartment, as previous reports suggested transportation of the proteasome along with the cytoskeleton[36,37].

This study characterized the aging of the proteasome, whereas its degradation process remains elusive. A recently published paper reported that plant proteasomes were degraded by autophagy[38]. However, knockdown of autophagy-related genes in the siRNA screen did not result in the delayed turnover (data not shown). This suggests that the role of autophagy in the constitutive degradation of the proteasome was undetectable in this assay or little at least in mammalian culture cells supplemented with sufficient nutrients.

Since the proteasome is a complex of 33 subunits, the turnover of Rpn11 might not always be followed by other subunits. However, almost all of the Rpn11 expressed in HeLa cells are incorporated into the 26S proteasome, and it is previously reported that the half-lives of 19S RP subunits and 20S CP subunits are almost the same, respectively[24,39]. This report suggests that the turnover of Rpn11 can at least represent that of 19S RP complex. Also, it is reasonable to speculate that the proteasome is not disassembled into each subunit but 19S RP and 20S CP complex are retained when the proteasome is degraded.

The functions of most of the identified genes shown in Fig 7C on the turnover of the proteasome are not explored yet. Although it is hard to predict the overall pathway of the degradation of the proteasome from this gene list, this might be helpful for further researches. To elucidate the detailed mechanism of the degradation of the proteasome in mammalian cells with a central focus on these genes is an issue in the future.

Materials and methods

Cell culture and reagents

Rpn11-Flag mouse embryonic fibroblasts (MEFs) were derived from Rpn11-Flag/EGFP tag-exchangeable knock-in mice (RBRC04949). MEFs and HeLa cells were cultured in Dulbecco's modified Eagle's Medium (DMEM) supplemented with 10% (MEFs) or 5% (HeLa) fetal bovine serum (FBS, Life Technologies), 100 U/ml penicillin, and 100 μg/ml streptomycin at 37ºC with 5% CO_2 incubation. Cre-recombinase was expressed in Rpn11-Flag MEFs via adenovirus or retrovirus. Adenovirus expressing Cre-recombinase was purified by Adeno-X Maxi Purification kit (Clontech). Vectors for retrovirus expressing Cre-recombinase and EGFP (pCLNCX NLS-Cre, pCLNCX EGFP, and pMD.G/vsv-g) were kindly provided by Hiroshi Nishina (Tokyo Medical and Dental University)[40]. Transfection was performed using Lipofectamine LTX & PLUS (for overexpression, Life technologies) or Lipofectamine RNAiMAX (for knockdown, Life technologies). The Sequences of the dsRNAs are as follows: negative control, 5'-AUGUAUUGGCCUGUAUUAGUU-3' and 5'-CUAAUACAGGCCAAUACAUUU-3'; AKAP8L, 5'-GCAAAUACCGGACCUUCUAUU-3' and 5'-UAGAAGGUCCGGUAUUUGCUU-3'; CSNK2A2, 5'-GGACAACUAUGACCAGCUUUU-3' and 5'-AAGCUGGUCAUAGUUGUCCUU-3'. For HaloTag labeling, cells were cultured in the medium mentioned above additionally supplemented with 100 nM Oregon Green, 10 nM TMR, or 10 μM bloking ligand Succinimidyl Ester (O4) for 15 min and washed by phosphate-buffered saline (PBS) twice. Succinimidyl Ester (O4) was incubated with 100 mM Tris-HCl (pH 8.0) for 60 min at 25ºC before use. To generate HeLa cells stably expressing Tet-On inducible Venus, HeLa cells were transfected with pCMV-Tet3G (Clontech) and were selected with 0.8 mg/ml G418. The selected cells were further transfected with pTRE3G-IRES (Clontech) encoding Venus and puromycin resistance gene, followed by 4 μg/ml puromycin selection.

Generation of Rpn11-Halo knock-in cells

Two CRISPR guide RNA (gRNA) sequences near the stop codon of human Rpn11 were chosen. Pairs of oligos for the site (GTAAACACTGGACAATATTTG, for clone #1) and (GTTCCTCCAAATGACGTTTG, for clone #2) was annealed, phosphorylated, and ligated into pX330 vector (Addgene)[32]. For homologous recombination, the targeting vector was constructed by inserting HaloTag and polyadenylation signal (pA) into 3' of human Rpn11

exon 12 with a puromycin resistance gene cassette the PGK promoter sequence and the pA of which were flanked at 5' and 3' end, respectively. Seven point mutations were introduced into the CRISPR-targeting sequences on the targeting vector. HeLa cells were transfected with the pX330 vector and the targeting vector using Lipofectamine LTX & PLUS, and then selected with 4 μg/ml puromycin. The genotypes of puromycin-resinstant colonies were determined by PCR analysis of extracted genomic DNA using the following primers:
5'-TGGTTCTGTTTTCTCTTTCC-3',
5'-CATTCCTTTAATGAAGCTACAGTAATACTCTCACC-3'.

Antibodies

The antibodies against Rpn1–3, Rpn6–8, Rpn10, Rpn13, Rpt1–6, β3, Uch37, Usp14, HHR23b, and PA28γ were described previously[41–45]. Polyclonal antibodies against Rpn5, Rpn9, Rpn11, Txnl1, EGFP, and HaloTag were raised in rabbits by using recombinant proteins as 6His fusion proteins of human Rpn5 (residues 1–161), human Rpn9 (full length), human Rpn11 (residues 171–287), human Txnl1 (residues 275–289), EGFP (full length), and HaloTag (full length), respectively. The antibody against Rpn12 was raised by immunizing guinea pig with human Rpn12 (full length). The antibodies for Ubiquitin (Dako Cytomation, Z 0458), Flag (Sigma, F1804), actin (Millipore, MAB1501R), α-tubulin (Santa Cruz, sc-5286), and GAPDH (Santa Cruz, sc-32233) were purchased from respective manufacturers.

Generation of specific antibodies against phosphorylated and unphosphorylated forms of Rpn3 at Ser 6

Phosphorylation-specific antibody against Rpn3 at Ser 6 was generated by immunization of a rabbit with phosphorylated peptide (MKQEGpSARRRGC) conjugated with keyhole limpet hemocyanin (KLH, Calbiochem), and then affinity purification and the removal of the fraction that reacted with unphosphorylated peptide (MKQEGSARRRGC) were performed using NHS-activated Sepharose 4 Fast Flow (GE Healthcare). Antibody against unphosphorylated Rpn3 at Ser 6 was raised in the similar way; the serum from a rabbit immunized by unphosphorylated peptide was subjected to affinity purification and antibodies that reacted with phosphorylated peptide were removed.

Immunoblotting and immunoprecipitation

Cells washed by PBS were lysed with ice-cold buffer A (25 mM Tris-HCl [pH 7.5], 0.2%

[v/v] NP-40, 1 mM dithiothreitol, 2 mM ATP, and 5 mM $MgCl_2$), and the extracts were clarified by centrifugation at 20,000 × g for 10 min at 4ºC. For phosphorylation assays, phosphatase inhibitor mix (5 mM NaF, 1 mM Na_3VO_4, 5 mM $Na_4P_2O_7$, and 10 mM β-glycerophosphate) was added into the buffer A. In the fractionation analysis, cells were first lysed with buffer B (25 mM HEPES-NaOH [pH 7.5], 10 mM KCl, and 5 mM $MgCl_2$) containing 1 μg/ml digitonin (Nacalai), and centrifuged at 1,000 × g for 5 min at 4ºC to generate supernatant (cytosolic fraction) and pellet. The pellet was dissolved with buffer B containing 1% (v/v) Triton-X100 and 1 U/ml Benzonase Nuclease (Novagen), and incubated on ice for 20 min, followed by centrifugation at 5,000 × g for 5 min at 4ºC to obtain clarified nuclear fraction. For immunoprecipitation, anti-Flag M2 agarose and Flag peptide were purchased from Sigma, and COSMOGEL Ig-Accept Protein G from Nacalai. For Western blotting, samples boiled with SDS sample buffer were subjected to SDS-PAGE, transferred to polyvinylidene fluoride membrane, incubated with Blocking One (Nacalai), and analyzed by immunoblotting. All images were taken with LAS 4000 (for immunoblotting, GE Healthcare) or Typhoon FLA 9000 (for fluorescence imaging, GE Healthcare) in the same settings and processed exactly the same way. Quantification of bands was performed using Fusion SL4 (M&S Instruments). Silver stain kit (Wako, 299-58901), OxyBlot kit (Millipore, S7150), and Phos-tag acrylamide (Wako, AAL-107) were purchased following the manufacturer's introductions.

Immunofluorescence

Cells were fixed with 4% paraformaldehyde (PFA) in PBS for 20 min at room temperature (RT), and permeabilized with 0.2% Triton-X100 in PBS. The permeabilized cells were incubated in blocking buffer (1% bovine serum albumin, 1% goat serum, 1% glycerol, and 0.2% [v/v] Triton-X100 in PBS) for 1 h at RT, and analyzed by immunostaining. The secondary antibody Alexa Fluor and the mountant ProLong Diamond were purchased from Life technologies. The images were obtained with TCS SP8 (Leica).

Assay of proteasome activity and glycerol gradient centrifugation analysis

To measure deubiquitinating activity, purified proteasomes in buffer A were incubated with ubiquitin-7-amido-4-methylcoumarin (Ub-AMC, LifeSensors) at 37ºC for 10 min. The emitted fluorescence was measured by 1420 ARVO MX (Perkin Elmer; excitation: 355 nm, emission: 460). Similarly, fluorescent peptide substrates purchased from Peptide Institute were used to measure chymotrypsin-like activity by

succinyl-Leu-Leu-Vl-Tyr-7-amido-4-methylcoumarin (Suc-LLVY-MCA), trypsin-like activity by t-butyloxycarbonyl-Leu-Arg-Arg (Boc-LRR)-MCA, and caspase-like activity by N-benzyloxycarbonyl-Leu-Leu-Glu (Z-LLE)-MCA, as described previously[30]. The degradation assay of recombinant ^{35}S-labeled ornithine decarboxylase (ODC) and ^{35}S-labeled polyubiquitinated cIAP1 protein was performed as described previously[46]. For glycerol gradient centrifugation analysis, clarified cell lysates were subjected to 8 to 32% (v/v) linear glycerol gradient centrifugation (22 h, 83,000 × g) and separated into 32 fractions, followed by measurement of peptidase activity of each fraction as described previously[46].

LC-MS/MS analysis of Rpn3

Identification of the phosphorylation site of Rpn3 was performed following the methods described in previous reports[47,48]. The CBB-stained bands corresponding Rpn3 were subjected to in-gel trypsin digestion and analyzed on Easy nLC 1000 coupled with Q-Exactive MS and nanoelectrospray ion source (Thermo Fisher Scientific). MS spectra were analyzed using Protein Discoverer (Thermo Fisher Scientific). The fragmentation spectra were searched against the UniProt database with the MASCOT search engine. Multiple alignment was carried out by Clustal Omega (1.2.1).

siRNA library and screening strategy

The human whole-genome siRNA library (Human Genome [G-005005], Human Druggable Subsets [G-004675], and Human Drug Target [G-004655]) from Thermo Fisher Scientific, covering siRNA targets for 18,151 genes in total with pools of four sequences per target gene, was dissolved in Ultra Pure Distilled Water (Life technologies) and 2.5 μl of 1 μM siRNA solution was dispensed into 384-well μClear cell culture microplates (Greiner 781090). Before cell seeding, siRNA on the assay plate was incubated with 0.1 μl of Lipofectamine RNAiMAX in 10 μl of Opti-MEM (Life technologies). Rpn11-Halo knock-in HeLa cells (clone #2) labeled with Oregon Green and the blocking ligand in 40 μl of culture medium were seeded onto the assay plate (1,500 cells per plate) and cultured. After 64 h, 10 μl of TMR solution in culture medium was added and then the cells were fixed by adding 10 μl of 10% PFA (final concentration: 1.6%) for 20 min at RT. PFA was removed by centrifugation, and the plate was washed by 80 μl of 25 mM Tris-HCl (pH 8.0). To stain nuclei, each well was filled with 40 μl of DAPI buffer (25 mM Tris-HCl [pH 8.0], 2% [w/v] triethylenediamine, and 500 ng/ml DAPI).

The cell images were obtained with CellInsight NXT (Thermo Fisher Scientific).

The cells were recognized by DAPI fluorescence, and subsequently the signal intensities of Oregon Green and TMR were quantified. To adjust positional effects, raw data was subjected to median polish using a statistical software R and Z* score of each targeted gene was calculated[33,49].

In the secondary screen, siRNA targets with two sequences per hit gene from the primary screen were analyzed. Rpn11-Halo knock-in HeLa cells were analyzed in the same way with the primary screen, but labeling of newly synthesized Rpn11-Halo just before PFA fixation was omitted. HeLa cells stably expressing Tet-On inducible Venus were cultured with 100 ng/ml doxycycline for 8 h, washed by PBS twice, and seeded onto the siRNA assay plates. In the flow cytometer assay, Rpn11-Halo knock-in HeLa cells cultured in 96-well plates were labeled in the same way with the primary screen. After TMR labeling, the cells were harvested by trypsinization, washed by flow cytometer buffer (1% FBS, 2 mM EDTA, and 0.02% NaN_3 in PBS), and subjected to measurement of fluorescence intensities by Attune NxT (Thermo Fisher Scientific). The scatter plot was drawn using FlowJo software.

Acknowledgments

I thank Shigeo Murata for supporting this work. I also thank Hiroshi Nishina for Cre-recombinase expression vectors, and Hidenori Ichijo and Isao Naguro for advice on generation of phosphorylation-specific antibodies and siRNA screen. Identification of the phosphorylation site was carried out under supervision of Yasushi Saeki and Hidehito Yoshihara. Global analysis of Rpn3 interactome was performed in collaboration with Shun-ichiro Iemura and Tohru Natsume. I am grateful to all the members of the Laboratory of Protein Metabolism, especially to Yuki Ohte and Yasuyuki Sakurai, for their valuable comments and technical support.

References

1. Finley, D. Recognition and Processing of Ubiquitin-Protein Conjugates by the Proteasome. *Annu. Rev. Biochem.* **78,** 477–513 (2009).
2. Murata, S., Yashiroda, H. & Tanaka, K. Molecular mechanisms of proteasome assembly. *Nat. Rev. Mol. Cell Biol.* **10,** 104–115 (2009).
3. Hirano, Y. *et al.* A heterodimeric complex that promotes the assembly of mammalian 20S proteasomes. *Nature* **437,** 1381–5 (2005).
4. Hirano, Y. *et al.* Cooperation of multiple chaperones required for the assembly of mammalian 20S proteasomes. *Mol. Cell* **24,** 977–84 (2006).
5. Borodovsky, A. *et al.* A novel active site-directed probe specific for deubiquitylating enzymes reveals proteasome association of USP14. *EMBO J.* **20,** 5187–96 (2001).
6. Hamazaki, J. *et al.* A novel proteasome interacting protein recruits the deubiquitinating enzyme UCH37 to 26S proteasomes. *EMBO J.* **25,** 4524–36 (2006).
7. Hiyama, H. *et al.* Interaction of hHR23 with S5a. The ubiquitin-like domain of hHR23 mediates interaction with S5a subunit of 26 S proteasome. *J. Biol. Chem.* **274,** 28019–25 (1999).
8. Mah, A. L., Perry, G., Smith, M. A. & Monteiro, M. J. Identification of ubiquilin, a novel presenilin interactor that increases presenilin protein accumulation. *J. Cell Biol.* **151,** 847–62 (2000).
9. Andersen, K. M. *et al.* Thioredoxin Txnl1/TRP32 is a redox-active cofactor of the 26 S proteasome. *J. Biol. Chem.* **284,** 15246–54 (2009).
10. Wiseman, R. L. *et al.* Thioredoxin-related Protein 32 is an arsenite-regulated Thiol Reductase of the proteasome 19 S particle. *J. Biol. Chem.* **284,** 15233–45 (2009).
11. Ravid, T. & Hochstrasser, M. Diversity of degradation signals in the ubiquitin-proteasome system. *Nat. Rev. Mol. Cell Biol.* **9,** 679–90 (2008).
12. Schwartz, A. L. & Ciechanover, A. Targeting proteins for destruction by the ubiquitin system: implications for human pathobiology. *Annu. Rev. Pharmacol. Toxicol.* **49,** 73–96 (2009).
13. Jakob, C. *et al.* Circulating proteasome levels are an independent prognostic factor for survival in multiple myeloma. *Blood* **109,** 2100–5 (2007).
14. Dennissen, F. J. A., Kholod, N. & van Leeuwen, F. W. The ubiquitin proteasome system in neurodegenerative diseases: culprit, accomplice or victim? *Prog. Neurobiol.* **96,** 190–207 (2012).

15. Arima, K. *et al.* Proteasome assembly defect due to a proteasome subunit beta type 8 (PSMB8) mutation causes the autoinflammatory disorder, Nakajo-Nishimura syndrome. *Proc. Natl. Acad. Sci. U. S. A.* **108,** 14914–9 (2011).
16. Vilchez, D. *et al.* RPN-6 determines C. elegans longevity under proteotoxic stress conditions. *Nature* **489,** 263–8 (2012).
17. Vilchez, D. *et al.* Increased proteasome activity in human embryonic stem cells is regulated by PSMD11. *Nature* **489,** 304–8 (2012).
18. Tonoki, A. *et al.* Genetic evidence linking age-dependent attenuation of the 26S proteasome with the aging process. *Mol. Cell. Biol.* **29,** 1095–106 (2009).
19. Sahara, K., Kogleck, L., Yashiroda, H. & Murata, S. The mechanism for molecular assembly of the proteasome. *Adv. Biol. Regul.* **54,** 51–8 (2014).
20. Huang, L. & Chen, C. H. Proteasome regulators: activators and inhibitors. *Curr. Med. Chem.* **16,** 931–9 (2009).
21. Aiken, C. T., Kaake, R. M., Wang, X. & Huang, L. Oxidative stress-mediated regulation of proteasome complexes. *Mol. Cell. Proteomics* **10,** R110.006924 (2011).
22. Cui, Z., Scruggs, S. B., Gilda, J. E., Ping, P. & Gomes, A. V. Regulation of cardiac proteasomes by ubiquitination, SUMOylation, and beyond. *J. Mol. Cell. Cardiol.* **71,** 32–42 (2014).
23. Tanaka, K., Mizushima, T. & Saeki, Y. The proteasome: molecular machinery and pathophysiological roles. *Biol. Chem.* **393,** 217–34 (2012).
24. Schwanhäusser, B. *et al.* Global quantification of mammalian gene expression control. *Nature* **473,** 337–42 (2011).
25. Sell, D. R., Strauch, C. M., Shen, W. & Monnier, V. M. 2-aminoadipic acid is a marker of protein carbonyl oxidation in the aging human skin: effects of diabetes, renal failure and sepsis. *Biochem. J.* **404,** 269–77 (2007).
26. Kinoshita, E., Kinoshita-Kikuta, E. & Koike, T. Separation and detection of large phosphoproteins using Phos-tag SDS-PAGE. *Nat. Protoc.* **4,** 1513–21 (2009).
27. Lander, G. C. *et al.* Complete subunit architecture of the proteasome regulatory particle. *Nature* **482,** 186–91 (2012).
28. Murakami, Y. *et al.* Ornithine decarboxylase is degraded by the 26S proteasome without ubiquitination. *Nature* **360,** 597–9 (1992).
29. Yang, Y., Fang, S., Jensen, J. P., Weissman, A. M. & Ashwell, J. D. Ubiquitin protein ligase activity of IAPs and their degradation in proteasomes in response to apoptotic stimuli. *Science* **288,** 874–7 (2000).

30. Murata, S. *et al.* Regulation of CD8+ T cell development by thymus-specific proteasomes. *Science* **316,** 1349–53 (2007).
31. Los, G. V *et al.* HaloTag: a novel protein labeling technology for cell imaging and protein analysis. *ACS Chem. Biol.* **3,** 373–82 (2008).
32. Cong, L. *et al.* Multiplex genome engineering using CRISPR/Cas systems. *Science* **339,** 819–23 (2013).
33. Zhang, X. D. Illustration of SSMD, z score, SSMD*, z* score, and t statistic for hit selection in RNAi high-throughput screens. *J. Biomol. Screen.* **16,** 775–85 (2011).
34. Natsume, T. *et al.* A direct nanoflow liquid chromatography-tandem mass spectrometry system for interaction proteomics. *Anal. Chem.* **74,** 4725–33 (2002).
35. Haarer, B., Aggeli, D., Viggiano, S., Burke, D. J. & Amberg, D. C. Novel interactions between actin and the proteasome revealed by complex haploinsufficiency. *PLoS Genet.* **7,** e1002288 (2011).
36. Gorbea, C. *et al.* A protein interaction network for Ecm29 links the 26 S proteasome to molecular motors and endosomal components. *J. Biol. Chem.* **285,** 31616–33 (2010).
37. Hsu, M.-T. *et al.* Stage-Dependent Axon Transport of Proteasomes Contributes to Axon Development. *Dev. Cell* **35,** 418–31 (2015).
38. Marshall, R. S., Li, F., Gemperline, D. C., Book, A. J. & Vierstra, R. D. Autophagic Degradation of the 26S Proteasome Is Mediated by the Dual ATG8/Ubiquitin Receptor RPN10 in Arabidopsis. *Mol. Cell* **58,** 1053–66 (2015).
39. Hendil, K. B. *et al.* The 20S proteasome as an assembly platform for the 19S regulatory complex. *J. Mol. Biol.* **394,** 320–8 (2009).
40. Uchida, Y. *et al.* Involvement of stress kinase mitogen-activated protein kinase kinase 7 in regulation of mammalian circadian clock. *J. Biol. Chem.* **287,** 8318–26 (2012).
41. Kaneko, T. *et al.* Assembly pathway of the Mammalian proteasome base subcomplex is mediated by multiple specific chaperones. *Cell* **137,** 914–25 (2009).
42. Uechi, H., Hamazaki, J. & Murata, S. Characterization of the testis-specific proteasome subunit α4s in mammals. *J. Biol. Chem.* **289,** 12365–74 (2014).
43. Hamazaki, J., Hirayama, S. & Murata, S. Redundant Roles of Rpn10 and Rpn13 in Recognition of Ubiquitinated Proteins and Cellular Homeostasis. *PLoS Genet.* **11,** e1005401 (2015).
44. Hamazaki, J. *et al.* Rpn10-mediated degradation of ubiquitinated proteins is essential for mouse development. *Mol. Cell. Biol.* **27,** 6629–38 (2007).
45. Moriishi, K. *et al.* Proteasome activator PA28gamma-dependent nuclear retention and

degradation of hepatitis C virus core protein. *J. Virol.* **77,** 10237–49 (2003).

46. Tomita, T. *et al.* Sirt1-deficiency causes defective protein quality control. *Sci. Rep.* **5,** 12613 (2015).
47. Tsuchiya, H., Tanaka, K. & Saeki, Y. The parallel reaction monitoring method contributes to a highly sensitive polyubiquitin chain quantification. *Biochem. Biophys. Res. Commun.* **436,** 223–229 (2013).
48. Koyano, F. *et al.* Ubiquitin is phosphorylated by PINK1 to activate parkin. *Nature* **510,** 162–6 (2014).
49. Brideau, C., Gunter, B., Pikounis, B. & Liaw, A. Improved Statistical Methods for Hit Selection in High-Throughput Screening. *J. Biomol. Screen.* **8,** 634–647 (2003).

Figure 1

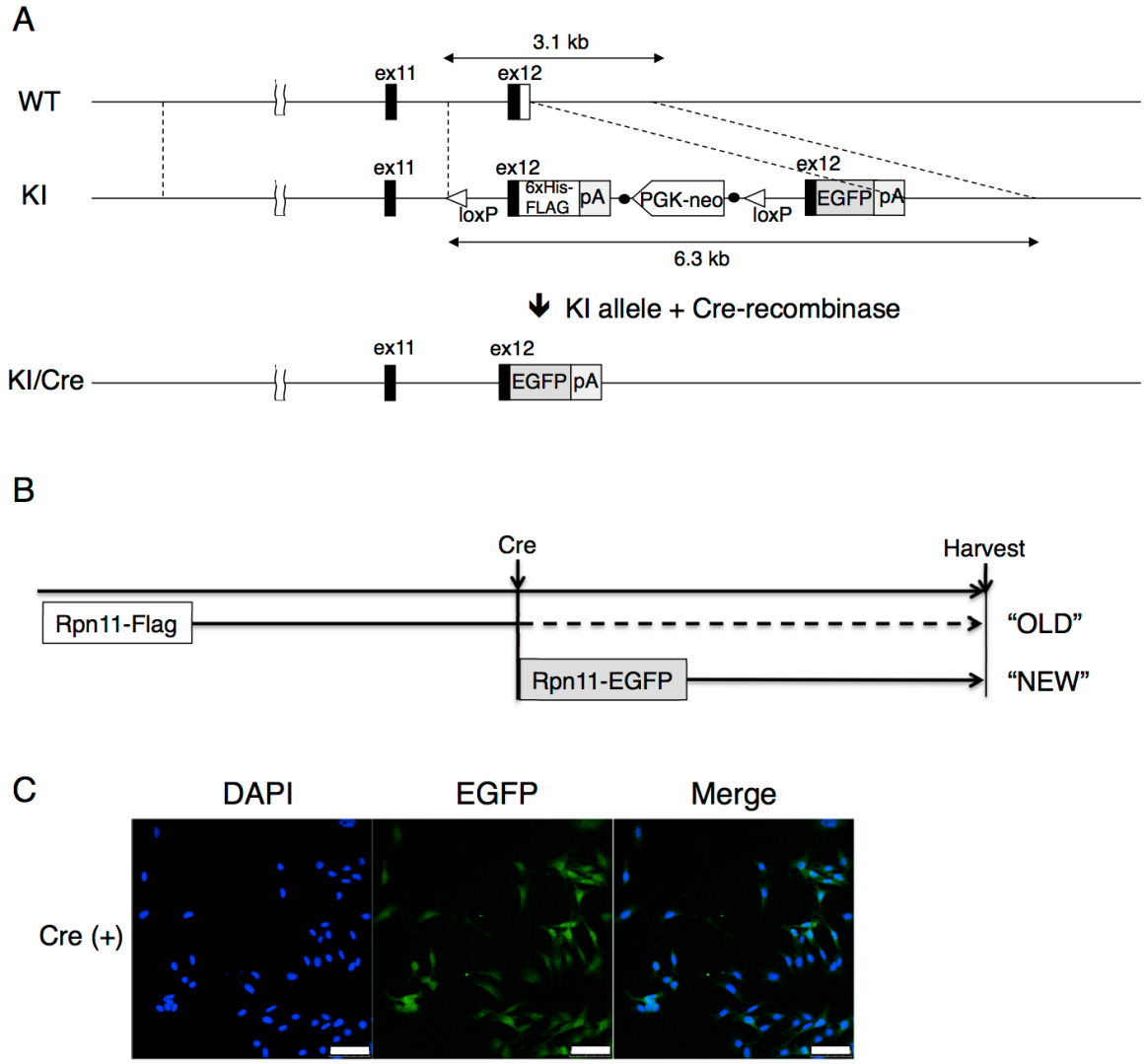

Figure 1. Materials for the purification of the old proteasome.

(A) Construct of Rpn11-Flag/EGFP tag-exchangeable knock-in mice. WT, KI, ex11, ex12, pA, PGK, and neo denote wild-type, knock-in, exon 11, exon 12, polyadenylation signal, PGK promoter sequence, and neomycin-resistant cassette, respectively.

(B) Concept of the old and the new proteasome.

(C) Rpn11-Flag MEFs were infected with adenovirus expressing Cre-recombinase, and after three days EGFP fluorescence was observed. Nuclei were stained with DAPI. Scale bar, 100 μm.

Figure 2

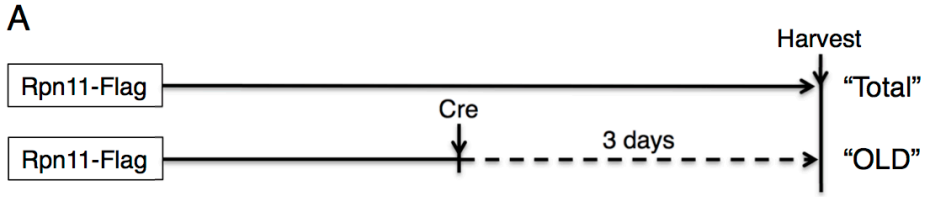
A
Harvest
Rpn11-Flag
"Total"
Cre
3 days
Rpn11-Flag
"OLD"

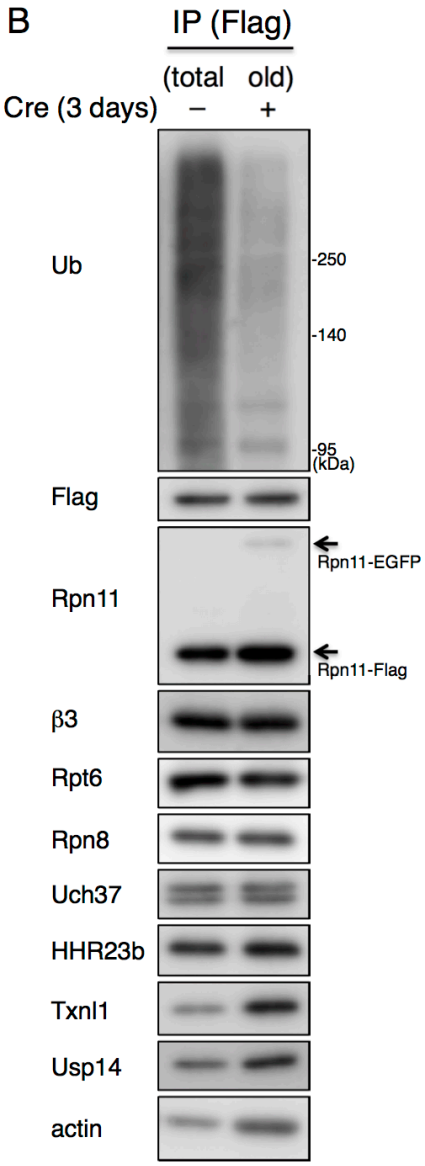
B
IP (Flag)
(total old)
Cre (3 days) – +
Ub
-250
-140
-95
(kDa)
Flag
Rpn11
Rpn11-EGFP
Rpn11-Flag
β3
Rpt6
Rpn8
Uch37
HHR23b
Txnl1
Usp14
actin

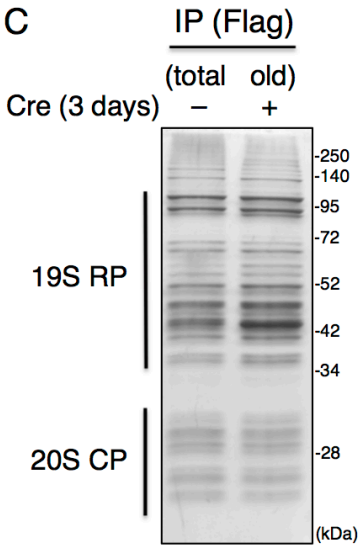
C
IP (Flag)
(total old)
Cre (3 days) – +
-250
-140
-95
-72
-52
-42
-34
-28
19S RP
20S CP
(kDa)

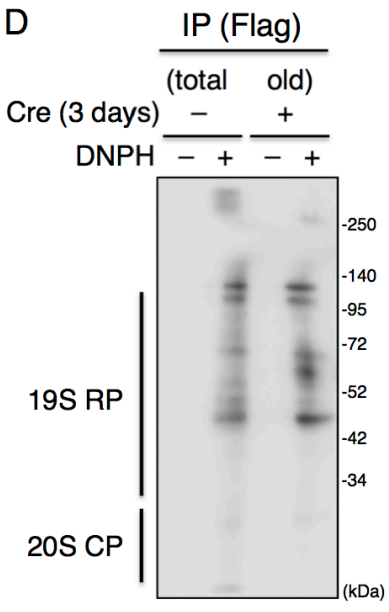
D
IP (Flag)
(total old)
Cre (3 days) – +
DNPH – + – +
-250
-140
-95
-72
-52
-42
-34
19S RP
20S CP
(kDa)

Figure 2. Purification of the old proteasome.

(A) The experimental scheme for the purification of the total and the old proteasome using Rpn11-Flag MEFs.

(B) Rpn11-Flag MEFs were infected with retrovirus expressing EGFP (control) or Cre-recombinase, and after three days the cells were harvested. Lysates were immunoprecipitated with anti-Flag antibodies, followed by Flag peptide elution. The samples were normalized by the protein level of Rpn11-Flag and subjected to immunoblotting with the indicated antibodies.

(C) Silver staining of the purified proteasome shown in (B).

(D) OxyBlot of the purified proteasome shown in (B). The carbonyl groups in the protein side chains were derivatized by reaction with 2,4-dinitrophenylhydrazine (DNPH).

Figure 3

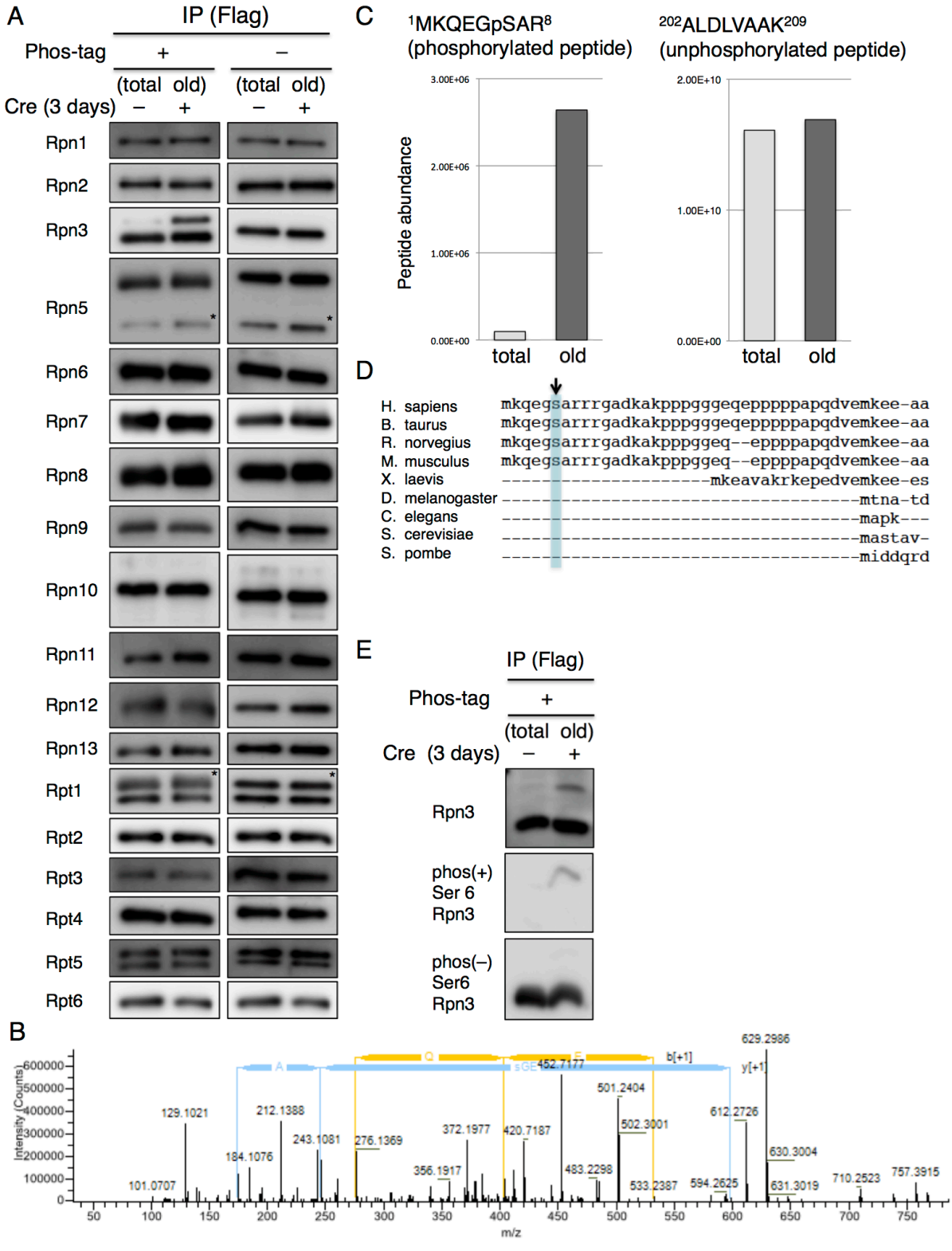
A
IP (Flag)
Phos-tag
+
–
(total old)
(total old)
Cre (3 days) – + – +
Rpn1
Rpn2
Rpn3
Rpn5
Rpn6
Rpn7
Rpn8
Rpn9
Rpn10
Rpn11
Rpn12
Rpn13
Rpt1
Rpt2
Rpt3
Rpt4
Rpt5
Rpt6
C
1MKQEGpSAR8
(phosphorylated peptide)
202ALDLVAAK209
(unphosphorylated peptide)
Peptide abundance
3.00E+06
2.00E+06
1.00E+06
0.00E+00
2.00E+10
1.00E+10
0.00E+00
total
old
D
H. sapiens mkqegsarrrgadkakpppgggeqeppppapqdvemkee-aa
B. taurus mkqegsarrrgadkakpppgggeqeppppapqdvemkee-aa
R. norvegius mkqegsarrrgadkakpppggeq--eppppapqdvemkee-aa
M. musculus mkqegsarrrgadkakpppggeq--eppppapqdvemkee-aa
X. laevis ----------mkeavakrkepedvemkee-es
D. melanogaster ----------mtna-td
C. elegans ----------mapk---
S. cerevisiae ----------mastav-
S. pombe ----------middqrd
E
IP (Flag)
Phos-tag
+
(total old)
Cre (3 days) – +
Rpn3
phos(+)
Ser 6
Rpn3
phos(–)
Ser6
Rpn3
B
Intensity (Counts)
m/z
b[+1]
y[+1]
452.7177
629.2986
501.2404
612.2726
502.3001
630.3004
631.3019
710.2523
757.3915
594.2625
533.2387
483.2298
420.7187
372.1977
356.1917
276.1369
243.1081
212.1388
184.1076
129.1021
101.0707

Figure 3. Phosphorylation of the old proteasome.

(A) Rpn11-Flag MEFs were infected with or without adenovirus expressing Cre-recombinase, and after three days the cells were harvested. Lysates were immunoprecipitated with anti-Flag antibodies, followed by Flag peptide elution. The samples were normalized by the protein level of Rpn11-Flag and loaded into SDS-PAGE with or without Phos-tag acrylamide, and subjected to immunoblotting with the indicated antibodies. Asterisks indicate non-specific bands.

(B) Mass spectrometric analysis of the tryptic phosphopeptide MKQEGpSAR from Rpn3.

(C) Relative quantification of MKQEGpSAR and ALDLVAAK peptides from Rpn3 in the total and the old proteasome.

(D) Multiple alignments of Rpn3 N-terminus.

(E) The purified proteasomes shown in Fig 2B were loaded into SDS-PAGE containing Phos-tag acrylamide, followed by immunoblotting with the indicated antibodies.

Figure 4

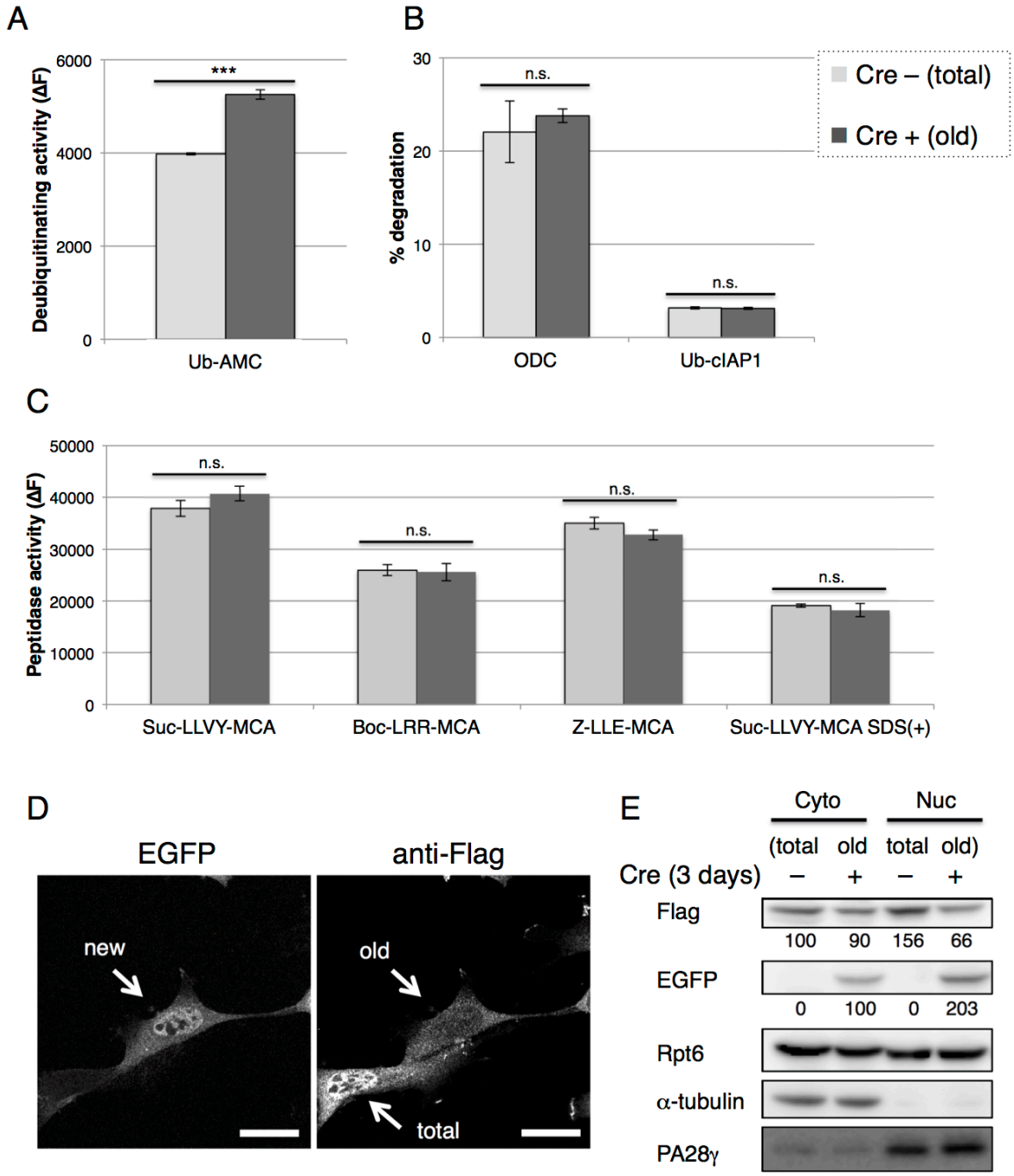
A
Deubiquitinating activity (ΔF)
6000
4000
2000
0
***
Ub-AMC
B
% degradation
30
20
10
0
n.s.
n.s.
ODC
Ub-cIAP1
Cre – (total)
Cre + (old)
C
Peptidase activity (ΔF)
50000
40000
30000
20000
10000
0
n.s.
n.s.
n.s.
n.s.
Suc-LLVY-MCA
Boc-LRR-MCA
Z-LLE-MCA
Suc-LLVY-MCA SDS(+)
D
EGFP
anti-Flag
new
old
total
E
Cyto
Nuc
(total old total old)
Cre (3 days) – + – +
Flag
100 90 156 66
EGFP
0 100 0 203
Rpt6
α-tubulin
PA28γ

Figure 4. Biochemical characterization of the old proteasome.

(A) Deubiquitinating activity of the proteasome. The purified proteasomes shown in Fig 2B were subjected to *in vitro* degradation assay using Ub-AMC as a substrate. The data represent means ± standard deviations (SD) from triplicate experiments. Statistical comparison was made by Student's t-test for two tailed unpaired samples. ***P < 0.001.

(B) Ubiquitin-independentand and -dependent protease activities of proteasomes. The purified proteasomes shown in Fig 2B were subjected to *in vitro* protein degradation assay. Antizyme-dependent degradation of ^{35}S-labeled ODC and ubiquitin-dependent degradation of ^{35}S-labeled cIAP1 were measured. The data represent means ± standard deviations (SD) from triplicate experiments. Statistical comparisons were made by Student's t-test for two tailed unpaired samples. n.s., not significant.

(C) Peptidase activities of the proteasome. The purified proteasomes shown in Fig 2B were subjected to *in vitro* degradation assay using Suc-LLVY-MCA, Boc-LRR-MCA, Z-LLE-MCA, and Suc-LLVY-MCA added with 0.025% SDS as substrates to assess the chymotrypsin-like, trypsin-like, caspase-like, and 20S CP activities, respectively. The data represent means ± standard deviations (SD) from triplicate experiments. Statistical comparisons were made by Student's t-test for two tailed unpaired samples. n.s., not significant.

(D) Immunofluorescence with anti-Flag antibody of Rpn11-Flag MEFs infected with adenovirus expressing Cre-recombinase for three days. Scale bar, 25 μm.

(E) Rpn11-Flag MEFs were infected with or without adenovirus expressing Cre-recombinase, and after three days the cells were harvested. Lysates were fractionated into cytosol and nucleus by digitonin treatement. α-tubulin and PA28γ serve as loading controls for cytosolic and nuclear fractions, respectively. Values represent the relative band intensities (normalized to Rpt6).

Figure 5

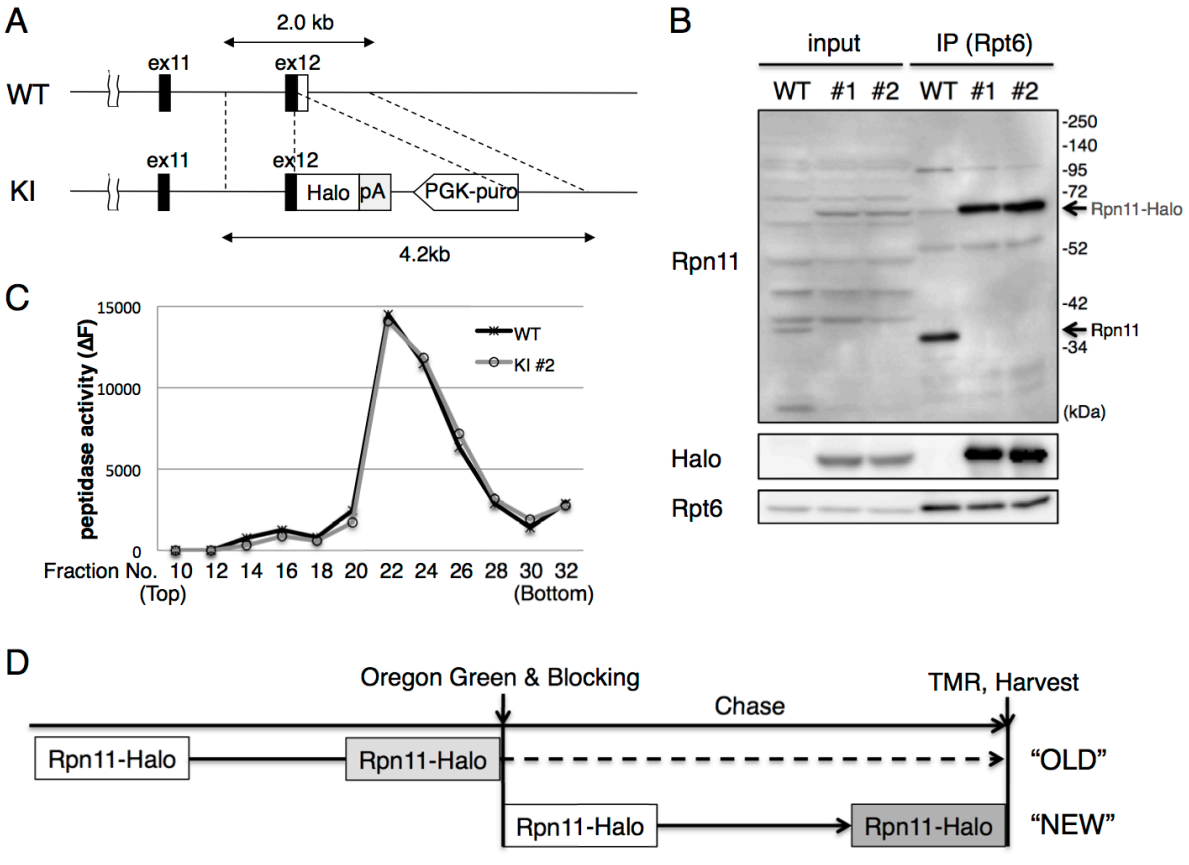
A
2.0 kb
ex11
ex12
WT
ex11
ex12
KI
Halo
pA
PGK-puro
4.2kb
B
input
IP (Rpt6)
WT #1 #2 WT #1 #2
-250
-140
-95
-72
Rpn11-Halo
-52
-42
Rpn11
-34
(kDa)
Rpn11
Halo
Rpt6
C
peptidase activity (ΔF)
15000
10000
5000
0
WT
KI #2
Fraction No. 10 12 14 16 18 20 22 24 26 28 30 32
(Top)
(Bottom)
D
Oregon Green & Blocking
Chase
TMR, Harvest
Rpn11-Halo
Rpn11-Halo
"OLD"
Rpn11-Halo
Rpn11-Halo
"NEW"
E
Chase 1 2 3 (days)
Oregon Green
TMR
Halo
GAPDH

Figure 5. Generation of Rpn11-Halo knock-in HeLa cells.

(A) Construct of Rpn11-Halo knock-in HeLa cells.

(B) Lysates from wild-type and Rpn11-Halo knock-in HeLa cells (clone #1 and #2) were subjected to immunoprecipitation with anti-Rpt6 antibodies, followed by immunoblotting with the indicated antibodies.

(C) Lysates from wild-type and Rpn11-Halo knock-in HeLa cells (clone #2) were fractionated by 8–32% glycerol gradient centrifugation. An aliquot of each fraction was used for an assay of chymotryptic activity of the proteasome using Suc-LLVY-AMC as a substrate.

(D) Schematic view of labeling the old and the new proteasome using Rpn11-Halo knock-in HeLa cells.

(E) Rpn11-Halo knock-in HeLa cells (clone #2) were labeled with Oregon Green ligands and subsequently subjected to the blocking ligand. After the indicated time, the cells were then labeled with TMR ligand. Harvested cells were kept frozen until they were lysed. Lysates were subjected to fluorescence imaging and immunoblotting. GAPDH serves as a loading control.

Figure 6

A

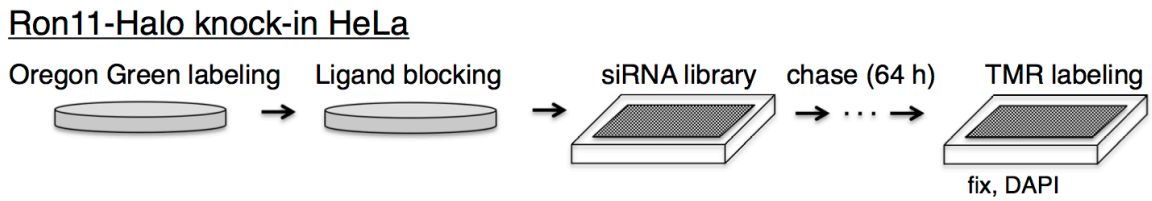
Ron11-Halo knock-in HeLa
Oregon Green labeling
Ligand blocking
siRNA library
chase (64 h)
TMR labeling
fix, DAPI

B

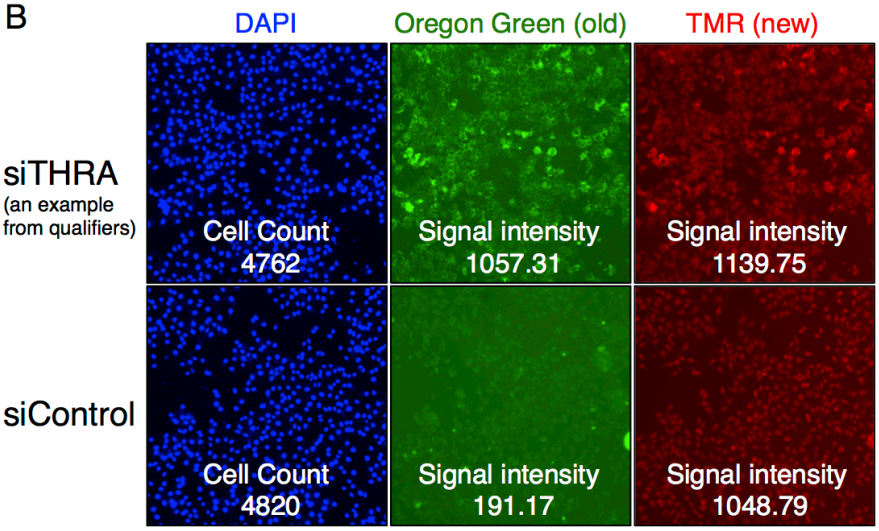
DAPI
Oregon Green (old)
TMR (new)
siTHRA
(an example
from qualifiers)
Cell Count
4762
Signal intensity
1057.31
Signal intensity
1139.75
siControl
Cell Count
4820
Signal intensity
191.17
Signal intensity
1048.79

C

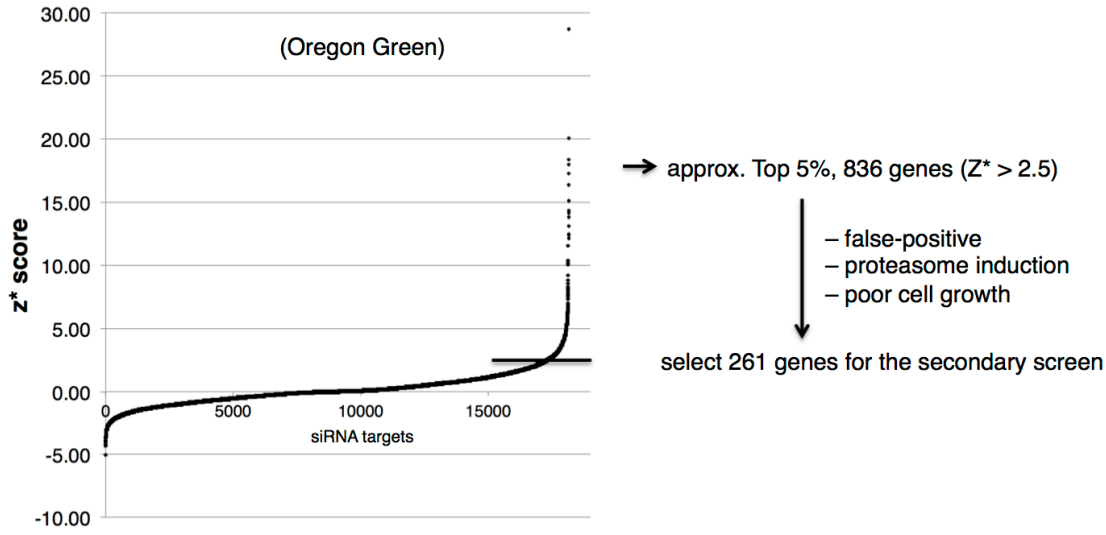
(Oregon Green)
z* score
30.00
25.00
20.00
15.00
10.00
5.00
0.00
-5.00
-10.00
0
5000
10000
15000
siRNA targets
approx. Top 5%, 836 genes (Z* > 2.5)
– false-positive
– proteasome induction
– poor cell growth
select 261 genes for the secondary screen

Figure 6. The primary screen for the identification of genes that affect the turnover of the proteasome.

(A) Schematic view of the primary screen using Rpn11-Halo knock-in HeLa cells.

(B) Examples of pictures analyzed in the primary screen.

(C) Graphical representation of the primary screen output and flow chart of procedures for selecting genes for the secondary screen.

Figure 7

A

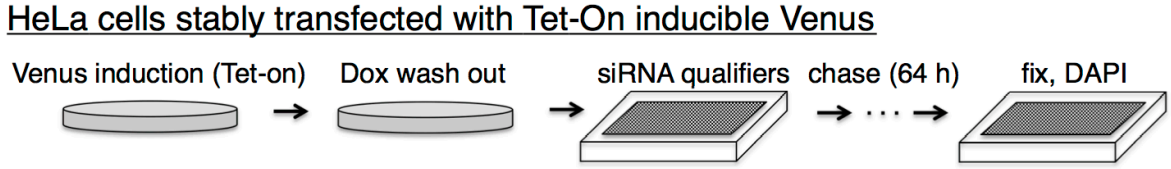

B

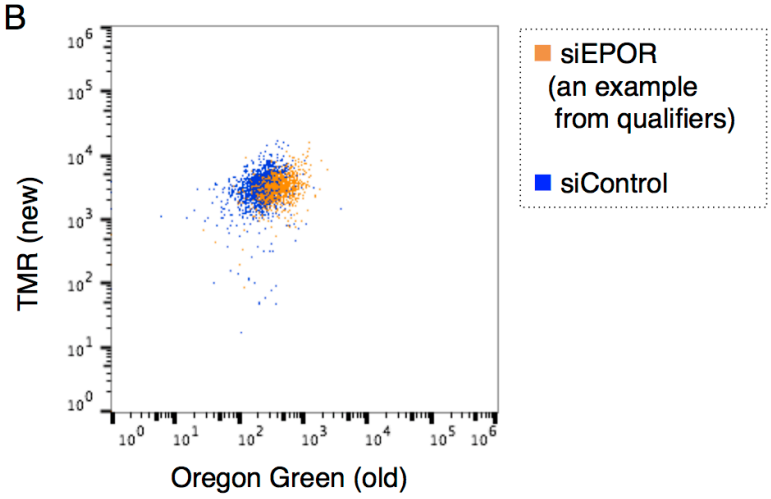

C

ARCN1	Coatomer subunit delta
EPOR	Erythropoietin receptor
CSNK2A2	Casein kinase II α' subunit
SORL1	Sortilin-related endocytic receptor
C6orf47	Uncharacterized protein
AKAP11	A-kinase (PKA) anchor protein 11
IFIT5	Interferon-induced protein
GBP5	Guanylate-binding protein 5
ANXA4	Annexin A4
AKAP8L	A-kinase (PKA) anchor protein 8-like

: kinase-related genes

Figure 7. The confirmation assays.

(A) Schematic view of the secondary screen using HeLa cells stably transfected with Tet-On inducible Venus. Dox, doxycycline.

(B) An example of the scatter plot from the flow cytometer assay.

(C) The list of genes identified by the screening.

Figure 8

A

Bait protein
nFlag Rpn3

HIT Preys

ADRM1	PSMA3	PSMD12
AFTPH	PSMA4	PSMD13
AKAP8L	PSMA5	PSMD14
CACYBP	PSMA6	PSMD2
CALU	PSMA7	PSMD4
CCDC47	PSMB1	PSMD6
DNAJB3	PSMB3	PSMD7
FKBP4	PSMB5	PSMD8
FKBP5	PSMB7	RCN2
GPRASP2	PSMC1	RNF219
HEATR5B	PSMC2	SAPS3
HUWE1	PSMC3	SIRT1
PPM1G	PSMC4	TCF25
PRKACA	PSMC5	TRIM26
PRKAR1A	PSMC6	UBE2H
PRKAR1B	PSMD1	UPF1
PSMA1	PSMD10	
PSMA2	PSMD11	

B

Bait protein
cFlag Rpn3

HIT Preys

ADRM1	PSMA6	PSMD2
AKAP8L	PSMA7	PSMD4
CACYBP	PSMB1	PSMD6
CCDC47	PSMB3	PSMD7
FKBP4	PSMB5	PSMD8
FKBP5	PSMB7	RCN2
GPRASP2	PSMC1	RNF219
HUWE1	PSMC2	SIRT1
PAAF1	PSMC3	TRIM26
PPM1G	PSMC4	UBB
PRKACA	PSMC5	UBE2H
PRKAR1A	PSMC6	
PRKAR1B	PSMD1	
PSMA1	PSMD10	
PSMA2	PSMD11	
PSMA3	PSMD12	
PSMA4	PSMD13	
PSMA5	PSMD14	

Figure 8. The interactome of Rpn3.

(A, B) Rpn3 tagged with Flag at its N-terminus (A) or C-terminus (B) were expressed in cells and anti-Flag immunoprecipitates were analysed by liquid chromatography coupled with tandem mass spectrometry.

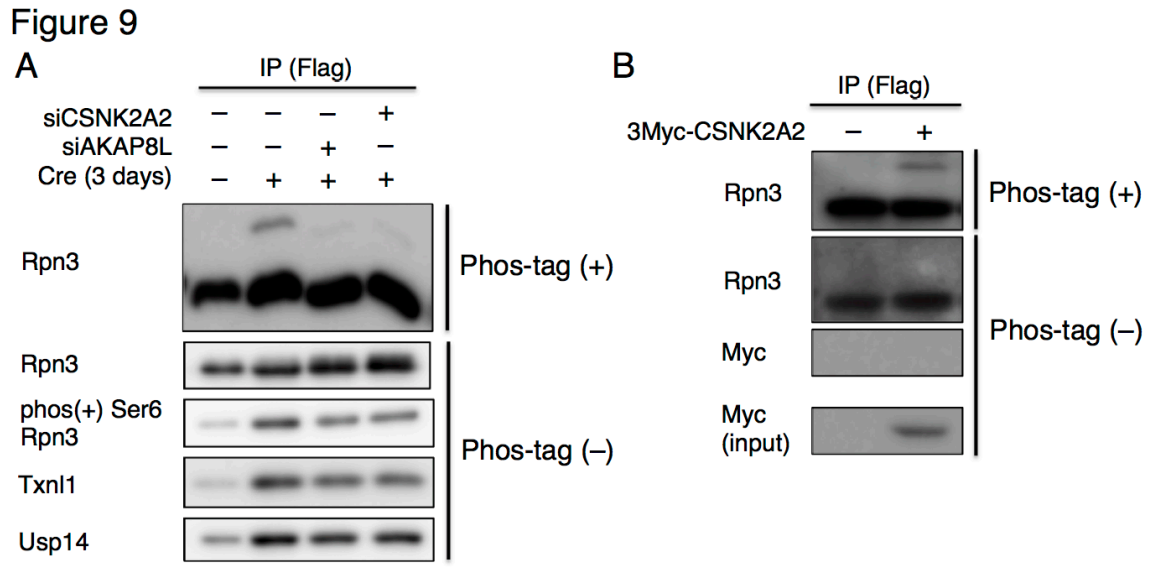

Figure 9. Phosphorylation of Rpn3 is regulated by AKAP8L and CSNK2A2.

(A) Negative control, AKAP8L, or CSNK2A2 knockdown for six days in Rpn11-Flag MEFs, followed by infection with or without adenovirus expressing Cre-recombinase for the last three days. Lysates were immunoprecipitated with anti-Flag antibodies, followed by Flag peptide elution. The samples were loaded into SDS-PAGE with or without Phos-tag acrylamide, and subjected to immunoblotting with the indicated antibodies.

(B) 3Myc-CSNK2A2 was overexpressed in Rpn11-Flag MEFs for 48 hours. Lysates were immunoprecipitated with anti-Flag antibodies. The samples were loaded into SDS-PAGE with or without Phos-tag acrylamide, and subjected to immunoblotting with the indicated antibodies.